

Sample-Specific Output Constraints for Neural Networks

Mathis Brosowsky Olaf Dünkler Daniel Slieter
Dr. Ing. h.c. F. Porsche AG
Weissach, Germany

mathis.brosowsky@porsche.de

olaf.duenkell@porsche.de

daniel.slieter@porsche.de

Marius Zöllner
FZI Research Center for Information Technology
Karlsruhe, Germany
zoellner@fzi.de

Abstract

Neural networks reach state-of-the-art performance in a variety of learning tasks. However, a lack of understanding the decision making process yields to an appearance as black box. We address this and propose ConstraintNet, a neural network with the capability to constrain the output space in each forward pass via an additional input. The prediction of ConstraintNet is proven within the specified domain. This enables ConstraintNet to exclude unintended or even hazardous outputs explicitly whereas the final prediction is still learned from data. We focus on constraints in form of convex polytopes and show the generalization to further classes of constraints. ConstraintNet can be constructed easily by modifying existing neural network architectures. We highlight that ConstraintNet is end-to-end trainable with no overhead in the forward and backward pass. For illustration purposes, we model ConstraintNet by modifying a CNN and construct constraints for facial landmark prediction tasks. Furthermore, we demonstrate the application to a follow object controller for vehicles as a safety-critical application. We submitted an approach and system for the generation of safety-critical outputs of an entity based on ConstraintNet at the German Patent and Trademark Office with the official registration mark DE10 2019 119 739.

1. Introduction

Deep neural networks have become state-of-the-art in many competitive learning challenges. The neural network acts as a flexible function approximator in an overall learning scheme. In supervised learning, the weights of the neural network are optimized by utilizing a representative set of valid input-output pairs. Whereas neural networks solve complex learning tasks [12] in this way, concerns arise ad-

ressing the black box character [6, 17]: (1) In general, a neural network represents a complex non-linear mapping and it is difficult to show properties for this function from a mathematical point of view, *e.g.* verification of desired input-output relations [2, 11] or inference of confidence levels in a probabilistic framework [5]. (2) Furthermore, the learned abstractions and processes within the neural network are usually not interpretable or explainable to an human [17].

With our approach, we address mainly the first concern: (1) We propose a neural network which predicts provable within a sample-specific constrained output space. *ConstraintNet* encodes a certain class of constraints, *e.g.* a certain type of a convex polytope, in the network architecture and enables to choose a specific constraint from this class via an additional input in each forward pass independently. In this way, *ConstraintNet* allows to enforce a consistent prediction with respect to a valid output domain. We assume that the partition into valid and invalid output domains is given by an external source. This could be a human expert, a rule based model or even a second neural network. (2) Secondly, we contribute to the interpretability and explainability of neural networks: A constraint over the output is interpretable and allows to describe the decision making of *ConstraintNet* in an interpretable way, *e.g.* later we model output constraints for a facial landmark prediction task such that the model predicts the facial landmarks on a region which is recognized as face and locates the positions of the eyes above the nose-landmark for anatomical reasons. Therefore, the additional input encodes the output constraint and represents high level information with explainable impact on the prediction. When this input is generated by a second model, it is an intermediate variable of the total model with interpretable information.

ConstraintNet addresses safety-critical applications in particular. Neural networks tend to generalize to new data

with high accuracy on average. However, there remains a risk of unforeseeable and unintended behavior in rare cases. Instead of monitoring the output of the neural network with a second algorithm and intervening when safety-critical behavior is detected, we suggest to constrain the output space with *ConstraintNet* to safe solutions in the first place. Imagine a neural network as motion planner. In this case, sensor detections or map data constrain the output space to only collision free trajectories.

Apart from safety-critical applications, *ConstraintNet* can be applied to predict within a region of interest in various use cases. *E.g.* in medical image processing, this region could be annotated by a human expert to restrict the localization of an anatomical landmark.

We demonstrate the modeling of constraints on several facial landmark prediction tasks. Furthermore, we illustrate the application to a follow object controller for vehicles as a safety-critical application. We have promising results on ongoing experiments and plan to publish in future.

2. Related work

In recent years, we observe an increasing attention in research addressing the black box character of neural networks. Apart from optimizing the data fitting and generalization performance of neural networks, in many applications it is important or even required to provide deeper information about the decision making process, *e.g.* in form of a reliable confidence level [5], an interpretation or even explanation [3, 18] or guarantees in form of proven mathematical properties [2, 11, 16]. Related research is known as Bayesian deep learning [5], interpretable and explainable AI [3, 6, 17, 18, 20, 21], adversarial attacks and defenses [2, 7, 15, 22], graph neural networks [1, 25], neural networks and prior knowledge [10] and verification of neural networks [2, 11, 16]. The approaches change the design of the model [1, 18, 20], modify the training procedure [2, 15] or analyze the behavior of a learned model after training [3, 11, 16, 21].

Verification and validation are procedures in software development to ensure the intended system behavior. They are an important concept of legally required development standards [23, 24] for safety-critical systems. However, it is difficult to transfer these guidelines to the development life-cycle of neural network based algorithms [19]. It is common practice to evaluate the neural network on an independent test set. However, the expressiveness of this validation procedure is limited by the finiteness of the test set. Frequently, it is more interesting to know if a property is valid for a certain domain with possibly infinite number of samples. These properties are usually input-output relations and express *e.g.* the exclusion of hazardous behavior [11], robustness properties [2] or consistency [10].

Verification approaches for neural networks [14] can be categorized in performing a reachability analysis [16], solv-

ing an optimization problem under constraints given by the neural network [2] or searching for violations of the considered property [9, 11]. Reluplex [11] is applicable to neural networks with ReLu-activation functions. It is a search based verification algorithm driven by an extended version of the simplex method. Huang *et al.* [9] perform a search over a discretized space with a stepwise refinement procedure to prove local adversarial robustness. Ruan *et al.* [16] reformulate the verification objective as reachability problem and utilize Lipschitz continuity of the neural network. Krishnamurthy *et al.* [2] solve a Lagrangian relaxed optimization problem to find an upper bound which represents depending on its value a safety certificate. This method interacts with the training procedure and rewards higher robustness in the loss function.

With *ConstraintNet*, we propose a neural network with the property to predict within sample-specific output domains. The property is guaranteed by the design of the network architecture and no subsequent verification process is required.

3. Neural networks with sample-specific output constraints

This section is structured as follows: (1) First of all, we define sample-specific output constraints and *ConstraintNet* formally. (2) Next, we propose our approach to create the architecture of *ConstraintNet*. This approach requires a specific layer without learnable parameters for the considered class of constraints. (3) We model this layer for constraints in form of convex polytopes and sectors of a circle. Furthermore, we derive the layer for constraints on different output parts. (4) Finally, we propose a supervised learning algorithm for *ConstraintNet*.

3.1. Sample-specific output constraints

Consider a neural network $n_\theta : \mathcal{X} \rightarrow \mathcal{Y}$ with learnable parameters $\theta \in \Theta$, input space \mathcal{X} and output space \mathcal{Y} .

We introduce an output constraint as a subset of the output space $\mathcal{C} \subset \mathcal{Y}$ and a class of output constraints as a parametrized set of them $\mathfrak{C} = \{\mathcal{C}(s) \subset \mathcal{Y} : s \in \mathcal{S}\}$. \mathcal{S} is here a set of parameters and we call an element $s \in \mathcal{S}$ constraint parameter. We define *ConstraintNet* as a neural network $f_\theta : \mathcal{X} \times \mathcal{S} \rightarrow \mathcal{Y}$ with the constraint parameter $s \in \mathcal{S}$ as an additional input and the guarantee to predict within $\mathcal{C}(s)$ by design of the network architecture, *i.e.* independently of the learned weights θ :

$$\forall \theta \in \Theta \forall s \in \mathcal{S} \forall x \in \mathcal{X} : f_\theta(x, s) \in \mathcal{C}(s). \quad (1)$$

Furthermore, we require that f_θ is (piecewise) differentiable with respect to θ so that backpropagation and gradient-based optimization algorithms are amenable.

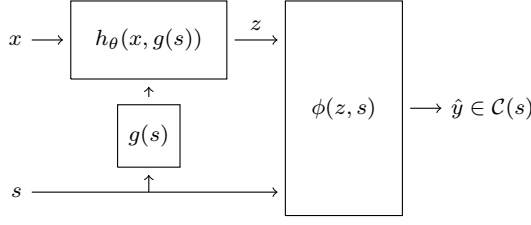


Figure 1. Approach to construct *ConstraintNet* for a class of constraints $\mathfrak{C} = \{\mathcal{C}(s) \subset \mathcal{Y} | s \in \mathcal{S}\}$. A final layer ϕ without learnable parameters maps the output of previous layers $z = h_\theta(x, g(s))$ on the constrained output space $\mathcal{C}(s)$ depending on the constraint parameter s . The previous layers h_θ get a representation $g(s)$ of s as an additional input to the data point x . This enables *ConstraintNet* to deal with different constraints for the same x .

3.2. Network architecture

Construction approach. We propose the approach visualized in Fig. 1 to create the architecture of *ConstraintNet* for a specific class of constraints \mathfrak{C} . The key idea is a final layer $\phi : \mathcal{Z} \times \mathcal{S} \rightarrow \mathcal{Y}$ without learnable parameters which maps the output of the previous layers $z \in \mathcal{Z}$ on the constrained output space $\mathcal{C}(s)$ depending on the constraint parameter s . Given a class of constraints $\mathfrak{C} = \{\mathcal{C}(s) \subset \mathcal{Y} : s \in \mathcal{S}\}$, we require that ϕ fulfills:

$$\forall s \in \mathcal{S} \forall z \in \mathcal{Z} : \phi(z, s) \in \mathcal{C}(s). \quad (2)$$

When ϕ is furthermore (piecewise) differentiable with respect to z we call ϕ constraint guard layer for \mathfrak{C} .

The constraint guard layer ϕ has no adjustable parameters and therefore the logic is learned by the previous layers h_θ with parameters θ . In the ideal case, *ConstraintNet* predicts the same true output y for a data point x under different but valid constraints. This behavior requires that h_θ depends on s in addition to x . Without this requirement, $z = h_\theta(\cdot)$ would have the same value for fixed x , and ϕ would project this z for different but valid constraint parameters s in general on different outputs. We transform s into an appropriate representation $g(s)$ and consider it as an additional input of h_θ , i.e. $h_\theta : \mathcal{X} \times g(\mathcal{S}) \rightarrow \mathcal{Z}$. For the construction of h_θ , we propose to start with a common neural network architecture with input domain \mathcal{X} and output domain \mathcal{Z} . In a next step, this neural network can be extended to add an additional input for $g(s)$. We propose to concatenate $g(s)$ to the output of an intermediate layer since it is information with a higher level of abstraction.

Finally, we construct *ConstraintNet* for the considered class of constraints \mathfrak{C} by applying the layers h_θ and the corresponding constraint guard layer ϕ subsequently:

$$f_\theta(x, s) = \phi(h_\theta(x, g(s)), s). \quad (3)$$

The required property for ϕ in Eq. 2 implies that *ConstraintNet* predicts within the constrained output space $\mathcal{C}(s)$ according to Eq. 1. Furthermore, the constraint guard layer propagates gradients and backpropagation is amenable.

Construction by modifying a CNN. Fig. 2 illustrates the construction of *ConstraintNet* by using a convolutional neural network (CNN) for the generation of the intermediate variable $z = h_\theta(x, g(s))$, where h_θ is a CNN. As an example, a nose landmark prediction task on face images is shown. The output constraints are triangles randomly located around the nose, i.e. convex polytopes with three vertices. Such constraints can be specified by a constraint parameter s consisting of the concatenated vertex coordinates. The constraint guard layer ϕ for convex polytopes is modeled in the next section and requires a three dimensional intermediate variable $z \in \mathbb{R}^3$ for triangles. The previous layers h_θ map the image data $x \in \mathcal{X}$ on the three dimensional intermediate variable $z \in \mathbb{R}^3$. A CNN with output domain $\mathcal{Z} = \mathbb{R}^{N_z}$ can be realized by adding a dense layer with N_z output neurons and linear activations. To incorporate the dependency of h_θ on s , we suggest to concatenate the output of an intermediate convolutional layer by a tensor representation $g(s)$ of s . Thereby, we extend the input of the next layer in a natural way.

3.3. Constraint guard layer for different classes of constraints

In this subsection we model the constraint guard layer for different classes of constraints. Primarily, we consider output constraints in form of convex polytopes. However, our approach is also applicable to problem-specific constraints. As an example, we construct the constraint guard layer for constraints in form of sectors of a circle. Furthermore, we model constraints for different parts of the output.

Convex polytopes. We consider convex polytopes \mathcal{P} in \mathbb{R}^N which can be described by the convex hull of M N -dimensional vertices $\{v^{(i)}\}_{i=1}^M$:

$$\mathcal{P}(\{v^{(i)}\}_{i=1}^M) = \left\{ \sum_i p_i v^{(i)} : p_i \geq 0, \sum_i p_i = 1 \right\}. \quad (4)$$

We assume that the vertices $v^{(i)}(s)$ are functions of the constraint parameter s and define output constraints via $\mathcal{C}(s) = \mathcal{P}(\{v^{(i)}(s)\}_{i=1}^M)$. The constraint guard layer for a class of these constraints $\mathfrak{C} = \{\mathcal{C}(s) : s \in \mathcal{S}\}$ can easily be constructed with $z \in \mathbb{R}^M$:

$$\phi(z, s) = \sum_i \sigma_i(z) v^{(i)}(s). \quad (5)$$

$\sigma_i(\cdot)$ denotes the i th component of the the M -dimensional softmax function $\sigma : \mathbb{R}^M \rightarrow \mathbb{R}^M$. The required property of ϕ in Eq. 2 follows directly from the properties $0 < \sigma_i(\cdot) < 1$ and $\sum_i \sigma_i(\cdot) = 1$ of the softmax function.

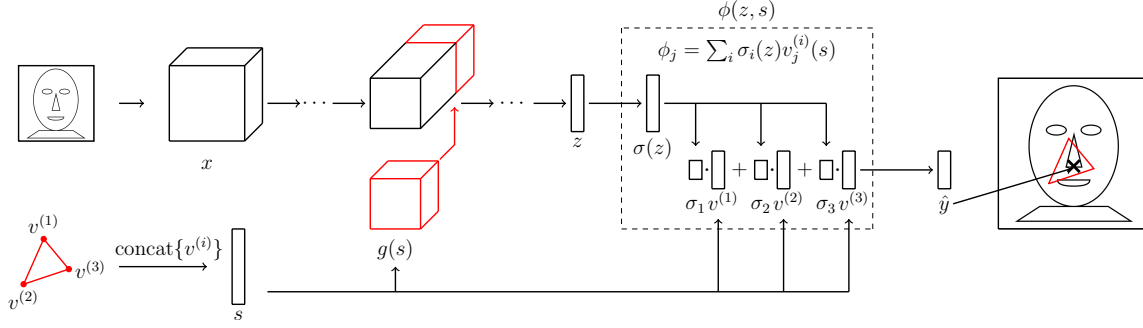


Figure 2. Construction of *ConstraintNet* by extending a CNN. For illustration purposes, we show a nose landmark prediction on an image x with an output constraint in form of a triangle, i.e. a convex polytope with three vertices $\{v^{(i)}(s)\}_{i=1}^3$. The constraint parameter s specifies the chosen constraint and consists in this case of concatenated vertex coordinates. A tensor representation $g(s)$ of s is concatenated to the output of an intermediate convolutional layer and extends the input of the next layer. Instead of creating the final output for the nose landmark with a 2-dimensional dense layer, a 3-dimensional intermediate representation z is generated. The constraint guard layer ϕ applies a softmax function σ on z and weights the three vertices of the triangle with the softmax outputs. This guarantees a prediction \hat{y} within the specified triangle.

However, some vertices $v^{(i)}$ might not be reachable exactly but upto arbitrary accuracy because $\sigma_i(\cdot) \neq 1$. Note that ϕ is differentiable with respect to z .

Sectors of a circle. Consider a sector of a circle \mathcal{O} with center position (x_c, y_c) and radius R . We assume that the sector is symmetric with respect to the vertical line $x = x_c$ and covers Ψ radian. Then the sector of a circle can be described by the following set of points:

$$\mathcal{O}(x_c, y_c, R, \Psi) = \{r \cdot (\sin \varphi, \cos \varphi) + (x_c, y_c) \in \mathbb{R}^2 : \\ r \in [0, R], \varphi \in [-\Psi/2, +\Psi/2]\}. \quad (6)$$

With $s = (x_c, y_c, R, \Psi)$, the output constraints can be written as $\mathcal{C}(s) = \mathcal{O}(x_c, y_c, R, \Psi)$. It is obvious that the following constraint guard layer with an intermediate variable $z \in \mathbb{R}^2$ fulfills Eq. 2 for a class of these constraints $\mathfrak{C} = \{\mathcal{C}(s) : s \in \mathcal{S}\}$:

$$\phi(z, s) = r(z_1) \cdot (\sin \varphi(z_2), \cos \varphi(z_2)) + (x_c, y_c), \quad (7)$$

$$r(z_1) = R \cdot \text{sig}(z_1), \quad (8)$$

$$\varphi(z_2) = \Psi \cdot (\text{sig}(z_2) - 1/2). \quad (9)$$

Note that we use the sigmoid function $\text{sig}(t) = 1/(1 + \exp(-t))$ to map a real number to the interval $(0, 1)$.

Constraints on output parts. We consider an output y with K parts $y^{(k)}$ ($k \in \{1, \dots, K\}$):

$$y = (y^{(1)}, \dots, y^{(K)}) \in \mathcal{Y} = \mathcal{Y}^{(1)} \times \dots \times \mathcal{Y}^{(K)}. \quad (10)$$

Each output part $y^{(k)}$ should be constrained independently to an output constraint $\mathcal{C}^{(k)}(s^{(k)})$ of a part-specific class of constraints:

$$\mathfrak{C}^{(k)} = \{\mathcal{C}^{(k)}(s^{(k)}) \subset \mathcal{Y}^{(k)} : s^{(k)} \in \mathcal{S}^{(k)}\}. \quad (11)$$

This is equivalent to constrain the overall output y to $\mathcal{C}(s) = \mathcal{C}^{(1)}(s^{(1)}) \times \dots \times \mathcal{C}^{(K)}(s^{(K)})$ with $s = (s^{(1)}, \dots, s^{(K)})$. The class of constraints for the overall output is then given by:

$$\mathfrak{C} = \{\mathcal{C}(s) \subset \mathcal{Y} : s \in \mathcal{S}^{(1)} \times \dots \times \mathcal{S}^{(K)}\}. \quad (12)$$

Assume that the constraint guard layers $\phi^{(k)}$ for the parts are given, i.e. for $\mathfrak{C}^{(k)}$. Then an overall constraint guard layer ϕ , i.e. for \mathfrak{C} , can be constructed by concatenating the constraint guard layers of the parts:

$$\phi(z, s) = (\phi^{(1)}(z^{(1)}, s^{(1)}), \dots, \phi^{(K)}(z^{(K)}, s^{(K)})), \quad (13)$$

$$z = (z^{(1)}, \dots, z^{(K)}). \quad (14)$$

The validity of the property in Eq. 2 for ϕ with respect to \mathfrak{C} follows immediately from the validity of this property for $\phi^{(k)}$ with respect to $\mathfrak{C}^{(k)}$.

3.4. Training

In supervised learning the parameters θ of a neural network are learned from data by utilizing a set of input-output pairs $\{(x_i, y_i)\}_{i=1}^N$. However, *ConstraintNet* has an additional input $s \in \mathcal{S}$ which is not unique for a sample. The constraint parameter s provides information in form of a region restricting the true output and therefore the constraint parameter s_i for a sample (x_i, y_i) could be any element of a set of valid constraint parameters $\mathcal{S}_{y_i} = \{s \in \mathcal{S} : y_i \in \mathcal{C}(s)\}$.

We propose to sample s_i from this set \mathcal{S}_{y_i} to create representative input-output pairs (x_i, s_i, y_i) . This sampling procedure enables *ConstraintNet* to be trained with standard supervised learning algorithms for neural networks. Note that many input-output pairs can be generated from the same data point (x_i, y_i) by sampling different constraint parameters s_i . Therefore, *ConstraintNet* is forced to learn

an invariant prediction for the same sample under different constraint parameters.

Algorithm 1 Training algorithm for *ConstraintNet*. The constraint parameter s_i for a data point (x_i, y_i) is sampled from a set of valid parameters $\mathcal{S}_{y_i} = \{s : y_i \in \mathcal{C}(s)\}$ to learn an invariant prediction for the same sample under different constraints.

```

procedure TRAIN( $\{x_i, y_i\}_{i=1}^N$ )
   $\theta \leftarrow$  random initialization  $\triangleright$  network weights
  for epoch  $\leftarrow 1$  to epochs do
    for batch  $\leftarrow 1$  to batches do
       $I_{batch} \leftarrow$  get_batch_indices(batch)
      for  $i \in I_{batch}$  do
         $\triangleright$  Sample from valid constraint parameters
         $s_i \leftarrow$  sample( $\mathcal{S}_{y_i}$ )
         $\hat{y}_i \leftarrow f_\theta(x_i, s_i)$   $\triangleright$  ConstraintNet
      end for
       $L(\theta) \leftarrow \frac{1}{|I_{batch}|} \sum_{i \in I_{batch}} l(y_i, \hat{y}_i) + \lambda R(\theta)$ 
       $\theta \leftarrow$  update( $\theta, \nabla_\theta L$ )
    end for
  end for
  return  $\theta$ 
end procedure

```

We train *ConstraintNet* with gradient-based optimization and sample s_i within the training loop as it is shown in Algorithm 1. The learning objective is given by:

$$\arg \min_{\theta} L(\theta) = \frac{1}{N} \sum_{i=1}^N l(y_i, \hat{y}_i) + \lambda R(\theta), \quad (15)$$

with $l(\cdot)$ being the sample loss, $R(\cdot)$ a regularization term and λ a weighting factor. The sample loss term $l(y_i, \hat{y}_i)$ penalizes deviations of the neural network prediction \hat{y}_i from the ground truth y_i . We apply *ConstraintNet* to regression problems and use mean squared error as sample loss.

4. Applications

In this section, we apply *ConstraintNet* on a facial landmark prediction task and a follow object controller for vehicles. The output constraints for the facial landmark prediction task restrict the solution space to consistent outputs, whereas the constraints for the follow object controller help to prevent collisions and to avoid violations of legislation standards. We want to highlight that both applications are exemplary. The main goal is an illustrative demonstration for leveraging output constraints with *ConstraintNet* in applications.

4.1. Consistent facial landmark prediction

In our first application, we consider a facial landmark prediction for the nose (\hat{x}_n, \hat{y}_n), the left eye ($\hat{x}_{le}, \hat{y}_{le}$) and

the right eye ($\hat{x}_{re}, \hat{y}_{re}$) on image data. We assume that each image pictures a face. We introduce constraints to confine the landmark predictions for nose, left eye and right eye to a bounding box which might be given by a face detector. Then, we extend these constraints and enforce relative positions between landmarks such as *the eyes are above the nose*. These constraints are visualized in the top row of Fig. 3. The bottom row shows constraints for the nose landmark in form of a triangle and a sector of a circle. These constraints can be realized with the constraint guard layers in Eq. 5 and Eq. 7. However, they are of less practical relevance.

Modified CNN architecture. First of all, we define the output of *ConstraintNet* according to:

$$\hat{y} = (\hat{x}_n, \hat{x}_{le}, \hat{x}_{re}, \hat{y}_n, \hat{y}_{le}, \hat{y}_{re}), \quad (16)$$

and denote the x -coordinates $\hat{y}^{(k_x)}$ with $k_x \in \{1, 2, 3\}$ and the y -coordinates $\hat{y}^{(k_y)}$ with $k_y \in \{4, 5, 6\}$. *ConstraintNet* can be constructed by modifying a CNN according to Fig. 2 and Sec. 3.2. E.g. ResNet50 [8] is a common CNN architecture which is used for many classification and regression tasks in computer vision [13]. In the case of regression, the prediction is usually generated by a final dense layer with linear activations. The modifications comprise adopting the output dimension of the final dense layer with linear activations to match the required dimension of z , adding the constraint guard layer ϕ for the considered class of constraints \mathcal{C} and inserting a representation $g(s)$ of the constraint parameter s at the stage of intermediate layers. We define $g(s)$ as tensor and identify channels $c \in \{1, \dots, \dim(s)\}$ with the components of the constraint parameter s , then we set all entries within a channel to a rescaled value of the corresponding constraint parameter component s_c :

$$g_{c,w,h}(s) = \lambda_c \cdot s_c, \quad (17)$$

$$w \in \{1, \dots, W\}, h \in \{1, \dots, H\}. \quad (18)$$

W and H denote the width and height of the tensor and each λ_c is a rescaling factor. We suggest to choose the factors λ_c such that s_c is rescaled to approximately the scale of the values in the output of the layer which is extended by $g(s)$.

Bounding box constraints. The bounding box is specified by a left boundary $l^{(x)}$, a right boundary $u^{(x)}$, a top boundary $l^{(y)}$ and a bottom boundary $u^{(y)}$. Note that the y -axis starts at the top of the image and points downwards. Confining the landmark predictions to a bounding box is equivalent to constrain $\hat{y}^{(k_x)}$ to the interval $[l^{(x)}, u^{(x)}]$ and $\hat{y}^{(k_y)}$ to the interval $[l^{(y)}, u^{(y)}]$ independently. These intervals are one dimensional convex polytopes with the interval boundaries as vertices. Thus, we can write the output constraints for the components with the definition in Eq. 4 as:

$$\mathcal{C}^{(k_x)}(s^{(k_x)}) = \mathcal{P}(\{l^{(x)}, u^{(x)}\}), \quad (19)$$

$$\mathcal{C}^{(k_y)}(s^{(k_y)}) = \mathcal{P}(\{l^{(y)}, u^{(y)}\}), \quad (20)$$

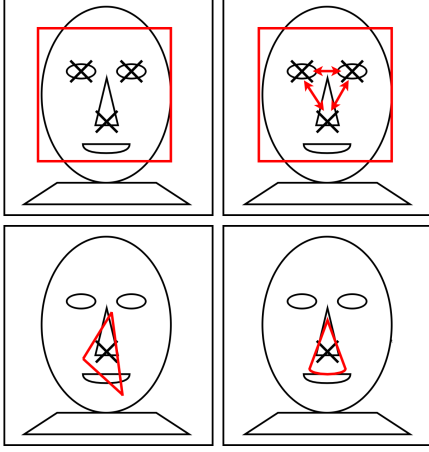


Figure 3. Top left: Landmark predictions for nose, left and right eye are confined to a bounding box around the face. Top right: In addition to the bounding box constraint, relations between landmarks are introduced, namely the eyes are above the nose and the left eye is in fact to the left of the right eye. Bottom: The nose landmark is constrained to a domain in form of a triangle (left) or a sector of a circle (right), respectively.

with $s^{(k_x)} = (l^{(x)}, u^{(x)})$ and $s^{(k_y)} = (l^{(y)}, u^{(y)})$. The constraint guard layers of the components are given by Eq. 5:

$$\phi^{(k_x)}(z^{(k_x)}, s^{(k_x)}) = \sigma_1(z^{(k_x)})l^{(x)} + \sigma_2(z^{(k_x)})u^{(x)}, \quad (21)$$

$$\phi^{(k_y)}(z^{(k_y)}, s^{(k_y)}) = \sigma_1(z^{(k_y)})l^{(y)} + \sigma_2(z^{(k_y)})u^{(y)}, \quad (22)$$

with $z^{(k_x)}, z^{(k_y)} \in \mathbb{R}^2$ and σ the 2-dimensional softmax function. Finally, the overall constraint guard layer $\phi(z, s)$ can be constructed from the constraint guard layers of the components according to Eq. 13 and requires a 12-dimensional intermediate variable $z \in \mathbb{R}^{12}$.

Enforcing relations between landmarks. We extend the bounding box constraints to model relations between landmarks. As an example, we enforce that the left eye is in fact to the left of the right eye ($\hat{x}_{le} \leq \hat{x}_{re}$) and that the eyes are above the nose ($\hat{y}_{le}, \hat{y}_{re} \leq \hat{y}_n$). These constraints can be written as three independent constraints for the output parts $\hat{y}^{(1)} = \hat{x}_n$, $\hat{y}^{(2)} = (\hat{x}_{le}, \hat{x}_{re})$, $\hat{y}^{(3)} = (\hat{y}_n, \hat{y}_{le}, \hat{y}_{re})$:

$$\mathcal{C}^{(1)}(s^{(1)}) = \{\hat{x}_n \in \mathbb{R} : l^{(x)} \leq \hat{x}_n \leq u^{(x)}\}, \quad (23)$$

$$\mathcal{C}^{(2)}(s^{(2)}) = \{(\hat{x}_{le}, \hat{x}_{re}) \in \mathbb{R}^2 : \hat{x}_{le} \leq \hat{x}_{re}, \\ l^{(x)} \leq \hat{x}_{le}, \hat{x}_{re} \leq u^{(x)}\}, \quad (24)$$

$$\mathcal{C}^{(3)}(s^{(3)}) = \{(\hat{y}_n, \hat{y}_{le}, \hat{y}_{re}) \in \mathbb{R}^3 : \hat{y}_{le}, \hat{y}_{re} \leq \hat{y}_n, \\ l^{(y)} \leq \hat{y}_n, \hat{y}_{le}, \hat{y}_{re} \leq u^{(y)}\}, \quad (25)$$

with constraint parameters $s^{(1)} = s^{(2)} = (l^{(x)}, u^{(x)})$ and $s^{(3)} = (l^{(y)}, u^{(y)})$. Fig. 4 visualizes the constraints for the output parts: $\mathcal{C}^{(1)}$ is a line segment in 1D, $\mathcal{C}^{(2)}$ is a triangle in 2D and $\mathcal{C}^{(3)}$ is a pyramid with 5 vertices in 3D. All of these are convex polytopes and therefore the constraint guard

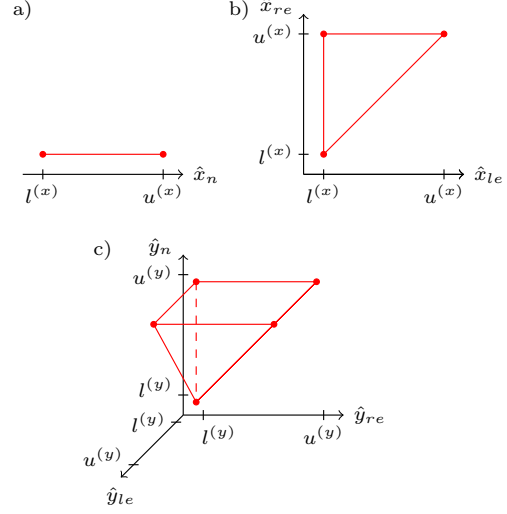


Figure 4. Confining landmark predictions for the nose (\hat{x}_n, \hat{y}_n), the left eye ($\hat{x}_{le}, \hat{y}_{le}$) and the right eye ($\hat{x}_{re}, \hat{y}_{re}$) to a bounding box with boundaries $l^{(x)}, u^{(x)}, l^{(y)}, u^{(y)}$, and enforcing that the eyes are above the nose ($\hat{y}_{le}, \hat{y}_{re} \leq \hat{y}_n$) and that the left eye is to the left of the right eye ($\hat{x}_{le} \leq \hat{x}_{re}$) is equivalent to constraining the output parts $\hat{y}^{(1)} = \hat{x}_n$ to the line segment a), $\hat{y}^{(2)} = (\hat{x}_{le}, \hat{x}_{re})$ to the triangle in b) and $\hat{y}^{(3)} = (\hat{y}_n, \hat{y}_{le}, \hat{y}_{re})$ to the pyramid in c).

layers for the parts $\{\phi^{(k)}\}_{k=1}^3$ are given by Eq. 5. Note that $\phi^{(k)}$ requires an intermediate variable $z^{(k)}$ with dimension equal to the number of vertices of the corresponding polytope. Finally, the overall constraint guard layer ϕ is given by combining the parts according to Eq. 13 and depends on an intermediate variable $z = (z^{(1)}, z^{(2)}, z^{(3)})$ with dimension $2+3+5=10$. Note that the introduced relations between the landmarks might be violated under rotations of the image and we consider them for demonstration purposes.

Training. For training of *ConstraintNet*, valid constraint parameters need to be sampled ($\text{sample}(\mathcal{S}_{y_i})$) according to Algorithm 1. To achieve this, random bounding boxes around the face which cover the considered facial landmarks can be created. *E.g.* in a first step, determine the smallest rectangle (parallel to the image boundaries) which covers the landmarks *nose*, *left eye* and *right eye*. Next, sample four integers from a given range and use them to extend each of the four rectangle boundaries independently. The sampled constraint parameter is then given by the boundaries of the generated box $l^{(x)}, u^{(x)}, l^{(y)}, u^{(y)}$. In inference, the bounding boxes might be given by a face detector.

4.2. Follow object controller with safety constraints

The adaptive cruise control (ACC) is a common driver assistance system for longitudinal control and available in many vehicles nowadays. A follow object controller (FOC) is part of the ACC and gets activated when a vehicle (target-

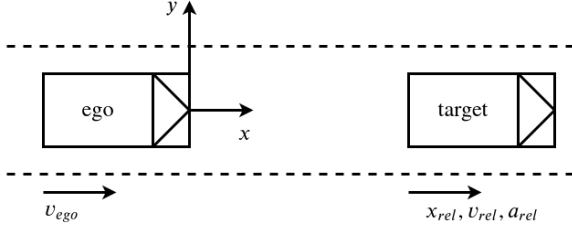


Figure 5. The follow object controller (FOC) in a vehicle (ego-vehicle) is only active when another vehicle (target-vehicle) is ahead. Sensors measure the velocity of the ego-vehicle v_{ego} and the relative position (distance) x_{rel} , the relative velocity v_{rel} and the relative acceleration a_{rel} of the target vehicle w.r.t. the coordinate system of the ego-vehicle. The FOC gets at least these sensor measurements as input and attempts to keep the distance to the target vehicle x_{rel} close to a velocity dependent distance $x_{rel, set}(v_{ego})$ under consideration of comfort and safety aspects. The output of the FOC is a demanded acceleration $a_{ego, dem}$.

vehicle) is ahead. This situation is visualized in Fig. 5. The output of the FOC is a demanded acceleration $a_{ego, dem}$ for the ego-vehicle with the goal to keep a velocity dependent distance $x_{rel, set}(v_{ego})$ to the vehicle ahead (target-vehicle) under consideration of comfort and safety aspects. Common inputs x for the FOC are sensor measurements such as the relative position (distance) x_{rel} , the relative velocity v_{rel} and the relative acceleration a_{rel} of the target vehicle w.r.t. the coordinate system of the ego-vehicle and the velocity v_{ego} of the ego-vehicle.

Modified fully connected network. The FOC is usually modeled explicitly based on expert knowledge and classical control theory. Improving the quality of the controller leads to models with an increasing number of separately handled cases, a higher complexity and a higher number of adjustable parameters. Finally, adjusting the model parameters gets a tedious work. This motivates the idea to implement the FOC as a neural network $a_{ego, dem} = n_{\theta}(x)$ and learn the parameters θ , e.g. in a reinforcement learning setting. Implementing the FOC with a common neural network comes at the expense of losing safety guarantees. However, with *ConstraintNet* $a_{ego, dem} = \pi_{\theta}(x, s)$ the demanded acceleration $a_{ego, dem}$ can be confined to a safe interval $[a_{min}, a_{max}]$ (convex polytope in 1D) in each forward pass independently. A *ConstraintNet* for this output constraint can be created by modifying a neural network with several fully connected layers. The output should be two dimensional such that the constraint guard layer in Eq. 5 for a 1D-polytope can be applied. For the representation $g(s)$ of the constraint parameter $s = (a_{min}, a_{max})$ rescaled values of the upper and lower bound are appropriate and can be added to the input. $g(s)$ is not inserted at an intermediate layer due to the smaller size of the network.

Constraints for safety. The output of *ConstraintNet* should be constrained to a safe interval $[a_{min}, a_{max}]$. The

interval is a convex polytope in 1D:

$$\mathcal{C}(s) = \mathcal{P}(\{a_{min}, a_{max}\}), \quad (26)$$

with $s = (a_{min}, a_{max})$. The constraint guard layer is given by Eq. 5. The upper bound a_{max} restricts the acceleration to avoid collisions. For deriving a_{max} , we assume that the target vehicle accelerates constantly with its current acceleration and the ego-vehicle continues its movement in the beginning with $a_{ego, dem}$. $a_{ego, dem}$ is then limited by the requirement that it must be possible to break without violating maximal jerk and deceleration bounds and without undershooting a minimal distance to the target-vehicle. Thus, a_{max} is the maximal acceleration which satisfies this condition. The maximal allowed deceleration for the ACC is given by a velocity dependent bound in ISO15622 [24] and would be an appropriate choice for a_{min} .

Training and reinforcement learning. In comparison to supervised learning, reinforcement learning allows to learn from experience, i.e. by interacting with the environment. The quality of the interaction with the environment is measured with a reward function and the interaction self is usually implemented with a simulator. The reward function can be understood as a metric for optimal behavior and the reinforcement learning algorithm learns a policy π_{θ} which optimizes the reward. In our case, $\pi_{\theta}(x, s)$ is the *ConstraintNet* for the FOC. Instead of sampling the constraint parameter s from a set of valid constraint parameters, exactly one valid s is computed corresponding to the safe interval $[a_{min}, a_{max}]$. Thereby, deep reinforcement learning algorithms for continuous control problems are applicable. One promising candidate is the Twin Delayed DDPG (TD3) algorithm [4]. Note that *ConstraintNet* leads to a collision free training, i.e. training episodes are not interrupted.

5. Conclusion

In this paper, we have presented an approach to construct neural network architectures with the capability to constrain the space of possible predictions in each forward pass independently. We call a neural network with such an architecture *ConstraintNet*. The validity of the output constraints has been proven and originates from the design of the architecture. As one of our main contributions, we presented a generic modeling for constraints in form of convex polytopes. Furthermore, we demonstrated the application of *ConstraintNet* on a facial landmark prediction task and a follow object controller for vehicles. The first application serves for demonstration of different constraint classes whereas the second shows how output constraints allow to address functional safety. We think that the developed methodology is an important step for the application of neural networks in safety-critical functions. We have promising results in ongoing work and plan to publish experimental results in future.

References

- [1] Thang D. Bui, Sujith Ravi, and Vivek Ramavajjala. Neural graph learning: Training Neural networks using graphs. In *WSDM 2018 - Proceedings of the 11th ACM International Conference on Web Search and Data Mining*, pages 64–71, 2018. [2](#)
- [2] Krishnamurthy Dvijotham, Sven Gowal, Robert Stanforth, Relja Arandjelovic, Brendan O’Donoghue, Jonathan Uesato, and Pushmeet Kohli. Training verified learners with learned verifiers. *arXiv preprint arXiv:1805.10265*, 2018. [1](#), [2](#)
- [3] Dumitru Erhan, Yoshua Bengio, Aaron Courville, and Pascal Vincent. Visualizing higher-layer features of a deep network. *University Montreal*, (1341):1–13, 2009. [2](#)
- [4] Scott Fujimoto, Herke Van Hoof, and David Meger. Addressing Function Approximation Error in Actor-Critic Methods. In *35th International Conference on Machine Learning, ICML 2018*, volume 4, pages 2587–2601. International Machine Learning Society (IMLS), 2018. [7](#)
- [5] Yarin Gal and Zoubin Ghahramani. Dropout as a Bayesian approximation: Representing model uncertainty in deep learning. In *33rd International Conference on Machine Learning*, volume 3, pages 1651–1660, 2016. [1](#), [2](#)
- [6] Leilani H. Gilpin, David Bau, Ben Z. Yuan, Ayesha Bajwa, Michael Specter, and Lalana Kagal. Explaining explanations: An overview of interpretability of machine learning. In *Proceedings - 2018 IEEE 5th International Conference on Data Science and Advanced Analytics, DSAA 2018*, pages 80–89, 2019. [1](#), [2](#)
- [7] Ian J. Goodfellow, Jonathon Shlens, and Christian Szegedy. Explaining and Harnessing Adversarial Examples. *International Conference on Learning Representations*, 2015. [2](#)
- [8] Kaiming He, Xiangyu Zhang, Shaoqing Ren, and Jian Sun. Deep residual learning for image recognition. In *Proceedings of the IEEE Computer Society Conference on Computer Vision and Pattern Recognition*, pages 770–778, 2016. [5](#)
- [9] Xiaowei Huang, Marta Kwiatkowska, Sen Wang, and Min Wu. Safety verification of deep neural networks. In *Lecture Notes in Computer Science (including subseries Lecture Notes in Artificial Intelligence and Lecture Notes in Bioinformatics)*, volume 10426 LNCS, pages 3–29, 2017. [2](#)
- [10] Anuj Karpatne, William Watkins, Jordan Read, and Vipin Kumar. Physics-guided Neural Networks (PGNN): An Application in Lake Temperature Modeling. *arXiv preprint arXiv:1710.11431*, 2017. [2](#)
- [11] Guy Katz, Clark Barrett, David L. Dill, Kyle Julian, and Mykel J. Kochenderfer. Reluplex: An efficient smt solver for verifying deep neural networks. *Lecture Notes in Computer Science (including subseries Lecture Notes in Artificial Intelligence and Lecture Notes in Bioinformatics)*, 10426 LNCS:97–117, 2017. [1](#), [2](#)
- [12] Alex Krizhevsky, Ilya Sutskever, and Geoffrey E. Hinton. ImageNet classification with deep convolutional neural networks. In *Advances in Neural Information Processing Systems*, 2012. [1](#)
- [13] Stéphane Lathuilière, Pablo Mesejo, Xavier Alameda-Pineda, and Radu Horaud. A Comprehensive Analysis of Deep Regression. *arXiv preprint arXiv:1803.08450*, 2018. [5](#)
- [14] Changliu Liu, Tomer Arnon, Christopher Lazarus, Clark Barrett, and Mykel J. Kochenderfer. Algorithms for Verifying Deep Neural Networks. *arXiv preprint arXiv:1903.06758*, 2019. [2](#)
- [15] Aleksander Madry, Aleksandar Makelov, Ludwig Schmidt, Dimitris Tsipras, and Adrian Vladu. Towards Deep Learning Models Resistant to Adversarial Attacks. *International Conference on Learning Representations*, 2017. [2](#)
- [16] Wenjie Ruan, Xiaowei Huang, and Marta Kwiatkowska. Reachability analysis of deep neural networks with provable guarantees. In *IJCAI International Joint Conference on Artificial Intelligence*, pages 2651–2659, 2018. [2](#)
- [17] Cynthia Rudin. Stop explaining black box machine learning models for high stakes decisions and use interpretable models instead. *Nature Machine Intelligence*, 1(5):206–215, 2019. [1](#), [2](#)
- [18] Sara Sabour, Nicholas Frosst, and Geoffrey E Hinton. Dynamic routing between capsules. In *Advances in Neural Information Processing Systems*, pages 3857–3867, 2017. [2](#)
- [19] Rick Salay, Rodrigo Queiroz, and Krzysztof Czarnecki. An Analysis of ISO 26262: Using Machine Learning Safely in Automotive Software. *arXiv preprint arXiv:1709.02435*, 2017. [2](#)
- [20] Sascha Saralajew, Lars Holdijk, Maike Rees, and Thomas Villmann. Prototype-based Neural Network Layers: Incorporating Vector Quantization. *arXiv preprint arXiv:1812.01214*, 2018. [2](#)
- [21] Karen Simonyan, Andrea Vedaldi, and Andrew Zisserman. Deep Inside Convolutional Networks: Visualising Image Classification Models and Saliency Maps. *arXiv preprint arXiv:1312.6034*, 2013. [2](#)
- [22] Christian Szegedy, Wojciech Zaremba, Ilya Sutskever, Joan Bruna, Dumitru Erhan, Ian Goodfellow, and Rob Fergus. Intriguing properties of neural networks. *arXiv preprint arXiv:1312.6199*, 2013. [2](#)
- [23] The International Organization for Standardization. Road vehicles Functional safety. *ISO 26262*, 2011. [2](#)
- [24] The International Organization for Standardization. Adaptive Cruise Control. *ISO15622*, 2018. [2](#), [7](#)
- [25] Jie Zhou, Ganqu Cui, Zhengyan Zhang, Cheng Yang, Zhiyuan Liu, Lifeng Wang, Changcheng Li, and Maosong Sun. Graph Neural Networks: A Review of Methods and Applications. *arXiv preprint arXiv:1812.08434*, 2018. [2](#)